

Pro64His (rs4644) polymorphism within galectin-3 is a risk factor of differentiated thyroid carcinoma and affects the transcriptome of thyrocytes engineered via CRISPR/Cas9 system.

Alda Corrado^{1*} PhD, Romina Aceto^{1,2*} MSc, Roberto Silvestri¹ MSc, Irene Dell'Anno¹ PhD, Benedetta Ricci³ MSc, Simona Miglietta⁴ MSc, Cristina Romei⁵ PhD, Roberto Giovannoni¹ Prof, Laura Poliseno⁶ PhD, Monica Evangelista⁶ MSc, Marianna Vitiello⁶ PhD, Monica Cipollini¹ PhD, Sonia Garritano⁷ PhD, Laura Giusti⁸ Prof, Lorenzo Zallocco MSc^{9,10}, Rossella Elisei^{5,*} Prof, Stefano Landi^{1,*} Prof, Federica Gemignani^{1,*} Prof

¹Department of Biology, Genetic Unit, University of Pisa, Via Derna 1, 56126, Pisa, Italy

²Humanitas Clinical and Research Centre- IRCCS, Via Manzoni 56, 20089, Milan, Italy

³Fondazione I.R.C.C.S., Istituto Neurologico Carlo Besta, Via Celoria 11, 20127, Milan, Italy

⁴San Raffaele Telethon Institute for Gene Therapy (SR-Tiget), IRCCS San Raffaele Scientific Institute, Via Olgettina 60, 20132, Milan, Italy

⁵Endocrine Unit, Department of Clinical and Experimental Medicine, University of Pisa, Via Paradisa 2, 56124, Pisa, Italy

⁶Institute of Clinical Physiology (IFC), CNR, Via Giuseppe Moruzzi 1, 56124, Pisa, Italy

⁷Centre for Integrative Biology, University of Trento, Via Sommarive 9, 38123, Trento, Italy.

⁸School of Pharmacy, University of Camerino, via Gentile III da Varano, 27 62032, Camerino, Italy

⁹Department of Biotechnology, Chemistry and Pharmacy, University of Siena, Viale Aldo Moro, 2, 53100, Siena, Italy;

¹⁰Department of Pharmacy, University of Pisa, Via Luca Ghini, 13, 56126, Pisa, Italy.

* These authors contributed equally to the paper

Email address:

Alda Corrado corradoalda@gmail.com; Romina Aceto romina.aceto93@gmail.com;

Roberto Silvestri r.silvestri17@gmail.com; Irene Dell'Anno

irene.dellanno@biologia.unipi.it; Benedetta Ricci benericci94@gmail.com; Simona

Miglietta miglietta.simona@hsr.it; Cristina Romei cristina.romei@unipi.it; Roberto

Giovannoni roberto.giovannoni@unipi.it; Laura Poliseno laura.poliseno@gmail.com;

Monica Evangelista m.evangelista@ifc.cnr.it; Marianna Vitiello mariannavitiello@live.it;
Monica Cipollini mcipollini@biologia.unipi.it; Sonia Garritano sonia.garritano@unitn.it;
Laura Giusti laura.giusti@unicam.it; Lorenzo Zallocco l.zallocco@gmail.com; Rossella Elisei
rossella.elisei@unipi.it; Stefano Landi slandi@biologia.unipi.it; Federica Gemignani
federica.gemignani@unipi.it

Running Title: Evaluation of SNP rs4644 in thyroid cancer

Key words: Galectin-3, differentiated thyroid carcinoma, CRISPR/Cas9, Transcriptome, RNA-seq, Functional polymorphism rs4644

Abstract

Background: Galectin-3 (*LGALS3*) is an important glycoprotein involved in the malignant transformation of thyrocytes acting in the extracellular matrix, cytoplasm and nucleus where it regulates TTF-1 and TCF4 transcription factors.

Within *LGALS3* gene, a common single nucleotide polymorphism (SNP) (c.191C>A, p.Pro64His; rs4644) encoding for the variant Proline to Histidine at codon 64 has been extensively studied. However, data on rs4644 in the context of thyroid cancer are lacking. Thus, the aim of the present work was to evaluate the role of the rs4644 SNP as risk factor for differentiated thyroid cancer (DTC) and to determine the effect on the transcriptome in thyrocytes.

Methods: A case-control association study in 1,223 controls and 1,142 unrelated consecutive DTC patients was carried out to evaluate the association between rs4644-P64H and the risk of DTC. We used the non-malignant cell line Nthy-Ori (rs4644-C/A) and the CRISPR/Cas9 technique to generate isogenic cells carrying either the rs4644-A/A or rs4644-C/C homozygosis. Then, the transcriptome of the derivative and unmodified parental cells was analyzed by RNA-seq. Genes differentially expressed were validated by RT-qPCR and further tested in the parental Nthy-Ori cells after *LGALS3* gene silencing, to investigate whether the expression of target genes was dependent on galectin-3 levels.

Results: Rs4644 AA genotype was associated with a reduced risk of DTC (compared to CC, $OR_{adj}=0.66$; 95%CI=0.46-0.93; $P_{ass}=0.02$). We found that rs4644 affects galectin-3 as transcriptional co-regulator. Among 34 genes affected by rs4644, *HES1*, *HSPA6*, *SPC24*, and *NHS* were of particular interest since their expression was rs4644-dependent (CC>AA for the first and AA>CC for the others) also in 574 thyroid tissues of GTex biobank (<https://gtexportal.org/home/index.html>). Moreover, the expression of these genes was regulated by *LGALS3*-silencing. Using the proximity ligation assay in Nthy-Ori cells we found TTF-1 interaction was genotype-dependent.

Conclusions: Our data shows that in thyroid rs4644 is a trans-expression quantitative trait locus that can modify the transcriptional expression of downstream genes, through the modulation of TTF-1.

Introduction

Genetics studies have shown several loci associated with predisposition to differentiated thyroid carcinoma (DTC) (1-6). However, these loci could explain only a small part of the attributable risk and more predisposing factors need to be explored (7). Within this context, galectin-3 (encoded by *LGALS3* gene) is an ideal candidate to be evaluated. This protein has a pivotal role in the regulation of basic cellular functions at the nuclear, cytoplasmic, and extracellular level (8). In normal human thyroid, the expression of galectin-3 is low or absent but it increases with tumor progression as occurs in other types of cancer (9-18).

For this reason, it was studied as an effective serum biomarker for DTC (19-21). The over-expression of galectin-3 is one of the drivers of the malignant transformation of several tissues, including thyroid (22-24). Thus, the activity of galectin-3 drew the interest of many researchers eliciting a large volume of studies mostly aimed at elucidating its role in the extracellular matrix (25, 26). However, in the nucleus, galectin-3 affects gene expression by regulating splicing (27, 28) and gene transcription (29, 30). However, galectin-3 is not a transcription factor (TF) but it binds to specific TFs and modulates their activities (31-34). In particular, in breast cancer cells galectin-3 interacts with the CRE/SP1 sites (32), TCF4 (33, 34), and with beta-catenin thereby activating Wnt signaling (35) and the transcription of important cancer genes (32, 34, 36). Nuclear galectin-3 was shown to be an important mediator of the beta-catenin/Wnt pathway also in thyroid cancer (TC) (37, 38). Furthermore, in TC cell lines galectin-3 interacts with TTF-1 (26) and co-localized with TCF4 to orchestrate the transcription of downstream genes involved in thyroid differentiation and proliferation (39, 40, 41). At codon 64 of galectin-3, there is a common genetic polymorphism (c.191C>A, p.Pro64His; rs4644) encoding for the variant Proline (P64) to Histidine (H64). Galectin-3 deprived breast cancer cells ectopically forced to express H64 or P64 showed that these isoforms are biochemically different. H64 could be cleaved by matrix metalloproteinases (MMPs) -2 and -9 and could bind to the endothelial cell surface with higher affinity as compared to P64. H64-expressing cells, when xenografted in a nude mouse model, also showed enhanced chemotaxis, angiogenesis, and formed larger tumors (42-45). Moreover, in case-control studies, rs4644 was associated with increased predisposition to breast (46), cervical (47), and prostate carcinoma (48).

The aim of the present work was to evaluate the role of rs4644 as a risk factor for DTC and its effects on the transcriptome in a model of thyrocytes engineered by the CRISPR/Cas9 system.

Material and Methods

Case-control association study: statistical power, subjects and genotyping

The case-control association study was carried out in 1,142 patients with DTC and 1,223 controls presenting consecutively to the University Hospital of Cisanello (Pisa, Italy). Volunteers gave their written informed consent and the study was approved by the local Ethical Committee. The interview of both cases and controls was carried out *via* a self-administered questionnaire, for collecting the main covariates at the time of blood samples being drawn. The genotyping was performed by the use of TaqMan assay. All the details are reported in the Supplementary File.

Cell cultures and gene editing

The non-malignant human thyroid cell line Nthy-ori-3-1 (Nthy-Ori; Sigma-Aldrich, Saint Louis, MO, USA) was employed for the *in vitro* assays and for gene editing. These cells, immortalized with SV40, were grown in medium RPMI 1640 supplemented with 10% FBS (EuroClone SpA, Milan, Italy).

Nthy-Ori cells have a heterozygote genotype C/A allowing the conversion into the homozygote genotypes (either A/A or C/C) with the CRISPR/Cas9 gene editing system in only one step. Gene edited cells were named ORI-AA, ORI-CC, and ORI-wild type (WT). All the experimental details for creation of the engineered cell lines are reported in the Supplementary File.

RNA-seq analysis and validation

Two independent experiments were performed. A total of 400 ng of RNA for each cell line was used to perform RNA-seq for profiling and comparing transcripts (by Eurofins Genomics S.r.L., Vimodrone, Milan). The reads from the three samples were aligned using human genome hg38 / GRC38, UCSC as reference (ANNOTATIONS: Gencode v22, Ensembl 80).

The statistically different RNA-seq genes were also validated by RT-qPCR using *beta-actin*, *GAPDH*, and *HPRT1* as reference genes. Data were analyzed with Bio-Rad CFX Manager 3.1.

The primer sequences are reported in Supplementary Table S1. All experiments were repeated three times.

Silencing of *LGALS3* and Western Blot analysis

The same genes analyzed by RT-qPCR in ORI-CC, ORI-AA, and ORI-WT cells were tested in unmodified Nthy-Ori cells following *LGALS3* gene silencing. Primers are reported in Supplementary Table S1. The silencing of *LGALS3* was performed by using 10nM of a pool of specific siRNAs for *LGALS3* (Qiagen, Valencia, CA, USA) (see Supplementary Table S1). AllStars siRNA (SI03650318) (Qiagen, Valencia, CA, USA) was used, at the same concentration, as negative control. Neon Transfection System (Thermo Fisher Scientific, Waltham, MA, USA) was used for siRNA electroporation following the manufacturer's protocol. Mouse primary monoclonal anti-LGALS3 (clone 1C1B2; Proteintech, Rosemont, USA; 1:2000) and anti-Actin (Clone C4, Millipore, MA, USA; 1:5000) were used as primary antibodies, while IgG-HRP (Santa Cruz Biotechnology, Santa Cruz, USA; 1:5000) was used as secondary antibody to test the silencing.

Furthermore, we evaluated the level of galectin-3 in ORI-AA and ORI-CC samples, according as previously described (49). Anti-galectin-3 antibody (Anti-galectin-3 (H160), SC-20157; Santa Cruz Biotechnology, inc, USA) was used at 1:1000 dilution. The immunocomplexes were detected using a HRP-conjugated secondary antibody (donkey anti-rabbit 1:10000) and the immunoblots were developed by using the ECL detection system. Details of the experimental methods are provided in the Supplementary File.

Proximity ligation assay (PLA) Protein-protein interaction was evaluated by PLA (Duolink kit, Sigma Aldrich, MO, USA) using specific antibodies to detect protein targets, and specific DNA primers linked to the antibodies. The multi-step assay included hybridization phase followed by DNA amplification with fluorescent probes. The amplified DNA was detected as dots, so a few interacting molecules can produce a visible signal, making the assay highly sensitive. We validated the interaction between galectin-3 and TTF-1 in ORI-AA, ORI-CC and ORI-WT cells. Primary antibodies against TTF-1 (Cell Signaling Technology; Rabbit 1:50) and galectin-3 (clone 1C1B2; Proteintech, Rosemont, USA; Mouse 1:100) were used. Dots were counted in twenty-five cells per cell line in two independent experiments.

***In silico* analyses**

Five hundred and seventy-four thyroid samples reported in GTEx portal (<https://GTExportal.org/home/>) were evaluated to determine any correlation between RNA-seq or RT-qPCR data and the different tissue-specific expression of genes. Relevant parameters were the Normalized Effect Size (NES), i.e. the slope of the linear regression calculated as the effect of the alternative allele, ALT, compared to the reference allele, REF, in the human genome, and the statistical significance of the regression analysis. The transcription factors binding sites within the promoters of the genes of interest were investigated by Gene Promoter Miner tool (<http://GPMiner.mbc.nctu.edu.tw/>).

Statistical analyses

The departure from the Hardy-Weinberg equilibrium was analysed with the χ^2 goodness-of-fit test (1 degree of freedom, type-I error=0.05). The association analysis was performed with multivariate logistic regression analysis. RNA-Seq reads were aligned and analyzed with TopHat and Cufflinks package. The genes differentially expressed were detected with cummeRbund package by applying the False Discovery Rate (FDR) correction. Details of these analyses are provided in the Supplementary File.

Results

In Figure S1, the flowchart summarizes how the study was carried out. The main results of the case-control association study are reported in Table 1. The population respected the Hardy-Weinberg equilibrium ($p=0.36$), and the controls (composed mainly by blood donors volunteers) showed a statistically significant older age than cases (52.98 vs 42.01) because the control group was mainly composed of volunteer blood donors. Increased risk of DTC was associated with sex (females vs males: $OR_{adj}=2.93$; 95%CI=2.53-3.79; $P_{ass}<10^{-6}$) and smoking habit (smokers vs non-smokers: $OR_{adj}=1.34$; 95%CI=1.13-1.59; $P_{ass}=8.00\times10^{-4}$) whereas, no differences were found by body mass index.

The uncommon homozygotes AA showed a statistically significant decreased risk of DTC ($OR_{adj}=0.66$; 95%CI=0.46-0.93; $P_{ass}=0.02$). The heterozygotes showed an intermediate risk with a MAX trend-test statistically significant for the additive model ($P_{trend}=4.21\times10^{-3}$). The papillary (PTC) and follicular (FTC) histotypes showed a similar trend with only PTC being statistically significant.

We studied whether the *LGALS3* rs4644-P64H variants could affect gene transcription. Therefore, Nthy-Ori cells carrying the desired genotypes were engineered by CRISPR/Cas9 (Figure 1). As control, a replicate of Nthy-Ori cells was subjected to the same process but without the administration of the donor DNA. Figure 2 shows the cDNA sequencing of the ORI-WT (panel A), of the ORI-CC (panel B), and of the ORI-AA (panel C). As shown in panel D, the splicing was unaffected by the persisting LoxP site within the intron III after the activation of the Cre recombinase. The same sequencing confirmed also the expression of the correct genotype. Furthermore, Western Blot showed that the total amount of galectin-3 was expressed at the same level in both the derivative cell lines (Figure S2).

The global transcriptomes of ORI-CC and ORI-AA cells were analysed by the RNA-seq. About 99% of the reads were mapped to the human reference *Homo sapiens* genome assembly GRCh38 (hg38) (Genome Reference Consortium; https://www.ncbi.nlm.nih.gov/assembly/GCF_000001405.26/). The gene expression for all the genes was compared between ORI-AA and ORI-CC cells (Figure 3) and 24 genes were differentially expressed (Table 2): 21 (Group A) showed an increased expression in ORI-AA as compared to ORI-CC cells, whereas 3 genes (Group B) had increased expression in the ORI-CC cells.

In order to increase the power of the study in detecting truly positive results, for replication we included extra 15 low-confidence genes. The first 8 were chosen because they showed both a statistical significance at nominal level of 0.05 and were known to be involved in thyroid carcinogenesis (Table 2, Group C: *NOTCH3*, *DNMT3B*, *CTGF*, *CRYAB*, *IL1A*, *TERC*, *TNFAIP6*, *DKK1*). The remaining 7 (Table 2, Group D: *C2orf16*, *CTB-32H22.1*, *DUSP6*, *HSPA6*, *NHS*, *SPC24*, *SPATA5*) were not statistically significant at any level but showed the highest differential expression (fold-change >3.00 or <-3.00, arbitrary threshold). The complete comparisons among cell lines are reported in Supplementary Table S2. The selected 39 genes underwent validation with RT-qPCR confirming the results of the RNA-seq analysis, with the exception of 5 genes in groups C and D, i.e. *HSPB8*, *TNFAIP6*, *CTB-32H22.1*, *DUSP6*, and *SPATA5* that displayed an opposite trend compared to the RNA-seq and were not considered further (Supplementary Table S3). In order to evaluate whether the expression of the remaining 34 genes could correlate with the number of variant alleles, a model of simple linear regression was used. The gene

expression level was considered as the dependent variable and the ORI-AA, ORI-WT, and ORI-CC cell lines (carrying 2, 1, and 0 variant alleles, respectively) as the independent quantitative variable. This analysis showed that the expression of 29 genes correlated with the allele dosage (Table 3), being the ORI-WT intermediate between ORI-AA and ORI-CC cells. The expression of the remaining 5 genes (*ANO2*, *GABBR1*, *RP11-672A2.1*, *C2orf16*, and *NHS*) in ORI-WT was similar to that found in ORI-AA or ORI-CC, suggesting that, in some cases, the state of heterozygosity behaves like homozygosity, as generally occurs in the dominant traits.

The parental Nthy-Ori cells were treated with control siRNA (siCtrl) or silenced with siLGALS3 (Supplementary Figure S3) and the mRNA expression of the 34 target genes was evaluated by RT-qPCR. Following *LGALS3* gene silencing, 22 genes showed a statistically significant differential expression after the correction for multiple testing, whereas 2, *CTGF* and *RNU1-27P*, were significant at the nominal level of $P=0.05$ (Figure 4).

When the promoters of the deregulated genes were analyzed, GPMiner showed 11 TFs in common (Supplementary Table S4). Among them, TTF-1 and TCF4 were the most interesting given their known interaction with galectin-3. By PLA, we showed that the interaction between TTF-1 and galectin-3 was genotype-dependent with average dots of 3.98 ± 0.36 for ORI-AA and 1.66 ± 0.65 for ORI-CC ($p\text{-value} = 0.04$) (Figure S4). We evaluated further the relationship between rs4644-P64H genotypes and the expression of the 22 target genes in 574 thyroid tissues using the Genotype-Tissue Expression (GTEx) project dataset (<https://gtexportal.org>). Our *in vitro* findings were confirmed for *HES1* ($P\text{-value} = 0.029$; normalized effect size, $NES = -0.083$), *HSPA6* ($P\text{-value} = 0.0097$; $NES = 0.095$), *NHS* ($P\text{-value} = 0.027$; $NES = 0.087$), and *SPC24* ($P\text{-value} = 0.031$; $NES = 0.098$) (Figure S5).

Discussion

We analyzed the rs4644 SNP, that is completely conserved across phylogenetically distant organisms and predicted by previous studies (42-44) to affect the activity of the encoded galectin-3. We found that the A-allele (H64) was associated with a statistically significant decreased risk of DTC following adjustment for covariates. This SNP was found to be associated with the risk of prostate, cervical, breast, and gastric carcinoma, and glioma (35, 37-39, 50, 51). In particular, in prostate cancer and glioma, the A-allele showed a protective effect as observed here in DTC (48, 51).

Since nuclear galectin-3 co-regulates gene expression, we determined whether there could be differences in gene regulation due to rs4644, providing a rationale for the predisposition to DTC. We found 39 genes were differentially expressed, most of them were dependent on the allele dosage. These genes belong to processes (apoptosis: *BIRC3*, *BAG3*, *HSPA1B*; angiogenesis: *C3*, *HSPB1*; adhesion: *C3*, *SPP1*, *EGR1*) or signaling pathways (beta-catenin/Wnt: *NFATC4*, *C3*; MAPK: *DUSP6*, *IL1A*, *HSPA6*, *HSPA1B*, *HSPB1*; PI3K-Akt: *SPP1*; TNF: *BIRC3*) often deregulated in tumors.

The CC-genotype was associated with increased expression of genes related to initiation and progression of pancreas ductal adenocarcinoma (*HES1*) (52), endometrial carcinoma (*ANO2*) (53), prostate/skin/kidney cancer (*EGR1*) (54, 55) and thyroid carcinoma (*DUSP6*) (56, 57). The protective AA-genotype was associated with increased expression of genes with anti-malignant effects in colorectal cancer (*GABBR1*) (58) and thyroid cancer (*NOTCH3*) (59), or with tumor suppressor activities (*CRYAB* and *IL1A*) (60-62). Among the 39 genes, 22 were shown to be also dependent upon the expression level of galectin-3 in gene silencing experiments.

The analysis of the promoter regions of the 22 genes showed that there are common binding sites for 11 transcription factors, among which were TTF-1 and TCF4. These are well-known TFs interacting with galectin-3 in the nucleus of thyrocytes (39). These previous observations were further corroborated by the PLA analysis, showing an increase in interaction between TTF-1 and galectin-3 in ORI-AA compared to the ORI-CC cells, providing the mechanism for the transcriptomic differences observed in the isogenic cell lines. Kim et al. (50) demonstrated that the germline variant H64 increases nuclear accumulation of beta-catenin promoting TCF4 transcriptional activity, reinforcing the notion that also TCF4 maybe involved in the interaction with galectin-3.

Further analysis, using the GTex portal of 574 thyroid tissues, confirmed that rs4644 A-allele was associated with reduced expression of *HSPA6*, *NHS* and *SPC24* while the C-allele with a higher expression of *HES1* supporting that the SNP behaves as a truly trans-eQTL. *HSPA6* is a molecular chaperone involved in the protection of the proteome from stress, and the folding and transport of newly synthesized polypeptides. A study of 552 DTC cases and 752 controls showed that SNP rs9427401 within *HSPA6* was associated with increased risk of DTC (63). *SPC24* is involved in the mitotic checkpoint pathway and TC tissues

showed high levels of the protein (64). *SPC24* knockdown in anaplastic thyroid cancer cell lines inhibited cell growth and invasiveness. In nude mice xenograft models these cells formed smaller tumors compared to *SPC24* expressing cells (64). *HES1* encodes for a transcriptional repressor involved in cell differentiation, proliferation, invasion, metastasis, and progression of several types of cancer including TC (65, 66). In thyroid-derived TPC-1, BCPAP, and 8505C cell lines, it has been shown that Hes1 belongs to the Notch signaling pathway, one of the most important pathways for the control of differentiation, proliferation, and apoptosis of thyrocytes (67, 68). *NOTCH3* expression, the most important regulator of the Notch pathway in thyroid (69), was found to be dependent on *LGALS3* genotypes and galectin-3 levels in our study.

In conclusion, *LGALS3* genotypes are associated with susceptibility to DTC. *LGALS3* genotypes lead to changes in the expression of downstream genes. H64 and P64 galectin-3 have different binding affinities for transcription factors, in particular for TTF-1 and TCF4.

Author Disclosure Statement

No competing financial interests exist.

Corresponding author:

Prof. Stefano Landi,

Department of Biology-Genetic Unit, University of Pisa

Via Derna, 1 56126, Pisa

Tel +39 0502211528; fax +39 0502211527

Email slandi@biologia.unipi.it

References

1. Olson E, Wintheiser G, Wolfe KM, Droessler J, Silberstein PT 2019 Epidemiology of Thyroid Cancer: A Review of the National Cancer Database, 2000-2013. *Cureus* 11:e4127.
2. Gudmundsson J, Sulem P, Gudbjartsson DF, Jonasson JG, Sigurdsson J, Bergthorsson JT, He H, Blondal T, Geller F, Jakobsdottir M, Magnusdottir DN, Matthiasdottir S, Stacey SN, Skarphedinsson OB, Helgadottir H, Li W, Nagy R, Aguillo E, Faure E, Prats E, Saez B, Martinez M, Eyjolfsson GI, Bjornsdottir US, Holm H, Kristjansson K, Frigge ML, Kristvinsson H, Gulcher JR, Jonsson T, Rafnar T, Hjartarsson H, Mayordomo JI, de la Chapelle A, Hrafnkelsson J, Thorsteinsdottir U, Kong A, Stefansson K 2009 Common variants on 9q22.33 and 14q13.3 predispose to thyroid cancer in European populations. *Nat Genet* 41:460–464.
3. Köhler A, Chen B, Gemignani F, Elisei R, Romei C, Figlioli G, Cipollini M, Cristaudo A, Bambi F, Hoffmann P, Herms S, Kalemba M, Kula D, Harris S, Broderick P, Houlston R, Pastor S, Marcos R, Velázquez A, Jarzab B, Hemminki K, Landi S, Försti A 2013 Genome-wide association study on differentiated thyroid cancer. *J Clin Endocrinol Metab* 98:E1674–E1681.
4. Wei WJ, Lu ZW, Wang Y, Zhu YX, Wang YL, Ji QH 2015 Clinical significance of papillary thyroid cancer risk loci identified by genome-wide association studies. *Cancer Genet* 208:68–75.
5. Świerniak M, Wójcicka A, Czetwertyńska M, Długosińska J, Stachlewska E, Gierlikowski W, Kot A, Górnicka B, Koperski L, Bogdańska M, Wiechno W, Jażdżewski K 2016 Association between GWAS-Derived rs966423 Genetic Variant and Overall Mortality in Patients with Differentiated Thyroid Cancer. *Clin Cancer Res* 22:1111–1119.
6. Figlioli G, Elisei R, Romei C, Melaiu O, Cipollini M, Bambi F, Chen B, Köhler A, Cristaudo A, Hemminki K, Gemignani F, Försti A, Landi S 2016 A Comprehensive Meta-analysis of Case-Control Association Studies to Evaluate Polymorphisms Associated with the Risk of Differentiated Thyroid Carcinoma. *Cancer Epidemiol Biomarkers Prev* 25:700–713.
7. Zuk O, Hechter E, Sunyaev SR, Lander ES 2012 The mystery of missing heritability: Genetic interactions create phantom heritability. *Acad Proc Natl Sci U S A* 109:1193–1198.

8. Sciacchitano S, Lavra L, Morgante A, Ulivieri A, Magi F, De Francesco GP, Bellotti C, Salehi LB, Ricci A 2018 Galectin-3: One Molecule for an Alphabet of Diseases, from A to Z. *Int J Mol Sci* 19:pii: E379.
9. Saussez S, Glinoe D, Chantrain G, Pattou F, Carnaille B, André S, Gabius H-J, Laurent G 2008 Serum galectin-1 and galectin-3 levels in benign and malignant nodular thyroid disease. *Thyroid* 18:705-712.
10. Li J, Vasilyeva E, Wiseman SM 2019 Beyond immunohistochemistry and immunocytochemistry: a current perspective on galectin-3 and thyroid cancer. *Expert Rev Anticancer Ther* 19:1017-1027.
11. Castronovo V, Van Den Brûle FA, Jackers P, Clausse N, Liu FT, Gillet C, Sobel ME 1996 Decreased expression of galectin-3 is associated with progression of human breast cancer. *J Pathol* 179:43-48.
12. van den Brule FA, Buicu C, Berchuck A, Bast RC, Deprez M, Liu FT, Cooper DN, Pieters C, Sobel ME, Castronovo V 1996 Expression of the 67-kD laminin receptor, galectin-1, and galectin-3 in advanced human uterine adenocarcinoma. *Hum Pathol* 27:1185-1191.
13. Irimura T, Matsushita Y, Sutton RC, Carralero D, Ohannesian DW, Cleary KR, Ota DM, Nicolson GL, Lotan R 1991 Increased content of an endogenous lactose-binding lectin in human colorectal carcinoma progressed to metastatic stages. *Cancer Res* 51:387-393.
14. Schoeppner HL, Raz A, Ho SB, Bresalier RS 1995 Expression of an endogenous galactose-binding lectin correlates with neoplastic progression in the colon. *Cancer* 75:2818-2826.
15. Song S, Ji B, Ramachandran V, Wang H, Hafley M, Logsdon C, Bresalier RS 2012 Overexpressed galectin-3 in pancreatic cancer induces cell proliferation and invasion by binding Ras and activating Ras signaling. *PLoS One* 7:e42699.
16. Lotan R, Belloni PN, Tressler RJ, Lotan D, Xu XC, Nicolson GL 1994 Expression of galectins on microvessel endothelial cells and their involvement in tumour cell adhesion. *Glycoconj J* 11:462-468.
17. Pacis RA, Pilat MJ, Pienta KJ, Wojno K, Raz A, Hogan V, Cooper CR 2000 Decreased galectin-3 expression in prostate cancer. *Prostate* 44:118-123.

18. Inohara H, Raz A 1994 Identification of human melanoma cellular and secreted ligands for galectin-3. *Biochem Biophys Res Commun* 201:1366-1375.
19. Xu XC, el-Naggar AK, Lotan R 1995 Differential expression of galectin-1 and galectin-3 in thyroid tumors. Potential diagnostic implications. *Am J Pathol* 147:815–822.
20. Danguy A, Camby I, Kiss R 2002 Galectins and cancer. *Biochem Biophys Acta* 1572:285–293.
21. Ito Y, Yoshida H, Tomoda C, Miya A, Kobayashi K, Matsuzuka F, Yasuoka H, Kakudo K, Inohara H, Kuma K, Miyauchi A 2005 Galectin-3 expression in follicular tumours: an immunohistochemical study of its use as a marker of follicular carcinoma. *Pathology* 37:296–298.
22. Elad-Sfadia G, Haklai R, Balan E, Kloog Y 2004 Galectin-3 augments K-Ras activation and triggers a Ras signal that attenuates ERK but not phosphoinositide 3-kinase activity. *J Biol Chem* 279:34922–34930.
23. Levy R, Grafi-Cohen M, Kraiem Z, Kloog Y 2010 Galectin-3 promotes chronic activation of K-Ras and differentiation block in malignant thyroid carcinomas. *Mol Cancer Ther* 9:2208–2219.
24. Shalom-Feuerstein R, Plowman SJ, Rotblat B, Ariotti N, Tian T, Hancock JF, Kloog Y 2008 K-ras nanoclustering is subverted by overexpression of the scaffold protein galectin-3. *Cancer Res* 68:6608-6616.
25. Domic J, Dabelic S, Flögel M 2006 Galectin-3: an open-ended story. *Biochim Biophys Acta* 1760:616–635.
26. Paron I, Scaloni A, Pines A, Bachi A, Liu FT, Puppini C, Pandolfi M, Ledda L, Di Loreto C, Damante G, Tell G 2003 Nuclear localization of Galectin-3 in transformed thyroid cells: a role in transcriptional regulation. *Biochem Biophys Res Commun* 302:545–553.
27. Dagher SF, Wang JL, Patterson RJ 1995 Identification of galectin-3 as a factor in pre-mRNA splicing. *Proc Natl Acad Sci U S A* 92:1213–1217.
28. Haudek KC, Spronk KJ, Voss PG, Patterson RJ, Wang JL, Arnoys EJ 2010 Dynamics of galectin-3 in the nucleus and cytoplasm. *Biochim Biophys Acta* 1800:181–189.
29. Fritsch K, Mernberger M, Nist A, Stiewe T, Brehm A, Jacob R 2016 Galectin-3 interacts with components of the nuclear ribonucleoprotein complex. *BMC Cancer* 16:502.

30. Nakahara S, Raz A 2007 Regulation of cancer-related gene expression by galectin-3 and the molecular mechanism of its nuclear import pathway. *Cancer Metastasis Rev* 26:605–610.
31. Song S, Byrd JC, Mazurek N, Liu K, Koo JS, Bresalier RS 2005 Galectin-3 modulates MUC2 mucin expression in human colon cancer cells at the level of transcription via AP-1 activation. *Gastroenterology* 129:1581–1591.
32. Lin HM, Pestell RG, Raz A, Kim HR 2002 Galectin-3 enhances cyclin D(1) promoter activity through SP1 and a cAMP-responsive element in human breast epithelial cells. *Oncogene* 21:8001–8010.
33. Liu FT, Rabinovich GA 2005 Galectins as modulators of tumour progression. *Nat Rev Cancer* 5:29–41.
34. Shimura T, Takenaka Y, Tsutsumi S, Hogan V, Kikuchi A, Raz A 2004 Galectin-3, a novel binding partner of beta-catenin. *Cancer Res* 64:6363–6367.
35. Lee YK, Lin TH, Chang CF, Lo YL 2013 Galectin-3 silencing inhibits epirubicin-induced ATP binding cassette transporters and activates the mitochondrial apoptosis pathway via β -catenin/GSK-3 β modulation in colorectal carcinoma. *PLoS One* 8:e82478.
36. Kim HR, Lin HM, Biliran H, Raz A 1999 Cell cycle arrest and inhibition of anoikis by galectin-3 in human breast epithelial cells. *Cancer Res* 59:4148–4154.
37. Weinberger PM, Adam BL, Gourin CG, Moretz 3rd WH, Bollag RJ, Wang BY, Liu Z, Lee JR, Terris DJ 2007 Association of nuclear, cytoplasmic expression of galectin-3 with beta-catenin/Wnt-pathway activation in thyroid carcinoma. *Arch Otolaryngol Head Neck Surg* 133:503–510.
38. Shimura T, Takenaka Y, Fukumori T, Tsutsumi S, Okada K, Hogan V, Kikuchi A, Kuwano H, Raz A 2005 Implication of galectin-3 in Wnt signaling. *Cancer Res* 65:3535–3537.
39. Gilbert-Sirieix M, Makoukji J, Kimura S, Talbot M, Caillou B, Massaad C, Massaad-Massade L 2011 Wnt/ β -catenin signaling pathway is a direct enhancer of thyroid transcription factor-1 in human papillary thyroid carcinoma cells. *PLoS One* 6:e22280.
40. Guazzi S, Price M, De Felice M, Damante G, Mattei MG, Di Lauro R 1990 Thyroid nuclear factor 1 (TTF-1) contains a homeodomain and displays a novel DNA binding specificity. *EMBO J* 9:3631–3639.

41. Takenaka Y, Inohara H, Yoshii T, Oshima K, Nakahara S, Akahani S, Honjo Y, Yamamoto Y, Raz A, Kubo T 2003 Malignant transformation of thyroid follicular cells by galectin-3. *Cancer Lett* 195:111–119.
42. Nangia-Makker P, Raz T, Tait L, Hogan V, Fridman R, Raz A 2007 Galectin-3 cleavage: a novel surrogate marker for matrix metalloproteinase activity in growing breast cancers. *Cancer Res* 67:11760–11768.
43. Nangia-Makker P, Wang Y, Raz T, Tait L, Balan V, Hogan V, Raz A 2010 Cleavage of galectin-3 by matrix metalloproteases induces angiogenesis in breast cancer. *Int J Cancer* 127:2530-2541.
44. Mazurek N, Byrd JC, Sun Y, Ueno S, Bresalier RS 2011 A galectin-3 sequence polymorphism confers TRAIL sensitivity to human breast cancer cells. *Cancer* 117:4375–4380.
45. Nangia-Makker P, Honjo Y, Sarvis R, Akahani S, Hogan V, Pienta KJ, Raz A 2000 Galectin-3 induces endothelial cell morphogenesis and angiogenesis. *Am J Pathol* 156:899-909.
46. Balan V, Nangia-Makker P, Schwartz AG, Jung YS, Tait L, Hogan V, Raz T, Wang Y, Yang ZQ, Wu GS, Guo Y, Li H, Abrams J, Couch FJ, Lingle WL, Lloyd RV, Ethier SP, Tainsky MA, Raz A 2008 Racial disparity in breast cancer and functional germ line mutation in galectin-3 (rs4644): a pilot study. *Cancer Res* 68:10045–10050.
47. Fang SQ, Feng YM, Li M 2017 Correlations of Galectin-3 Gene Polymorphisms with Risk and Prognosis of Cervical Cancer in Chinese Populations: A Case-Control Study. *Oncol Res Treat* 40:533-539.
48. Meyer A, Coinac I, Bogdanova N, Dubrowinskaja N, Turmanov N, Haubold S, Schürmann P, Imkamp F, von Klot C, Merseburger AS, Machtens S, Bremer M, Hillemanns P, Kuczyk MA, Karstens JH, Serth J, Dörk T 2013 Apoptosis gene polymorphisms and risk of prostate cancer: a hospital-based study of German patients treated with brachytherapy. *Urol Oncol* 31:74–81.
49. Ciregia F, Bugliani M, Ronci M, Giusti L, Boldrini C, Mazzoni MR, Mossuto S, Grano F, Cnop M, Marselli L, Giannaccini G, Urbani A, Lucacchini A, Marchetti P 2017 Palmitate-induced lipotoxicity alters acetylation of multiple proteins in clonal β cells and human pancreatic islets. *Sci Rep* 7:13445.

50. Kim SJ, Shin JY, Cheong TC, Choi IJ, Lee YS, Park SH, Chun KH 2011 Galectin-3 germline variant at position 191 enhances nuclear accumulation and activation of β -catenin in gastric cancer. *Clin Exp Metastasis* 28:743–750.
51. Lee YH, Song GG 2015 Genome-wide pathway analysis in glioma. *Neoplasma* 62:230-238.
52. Nishikawa Y, Kodama Y, Shiokawa M, Matsumori T, Marui S, Kuriyama K, Kuwada T, Sogabe Y, Kakiuchi N, Tomono T, Mima A, Morita T, Ueda T, Tsuda M, Yamauchi Y, Sakuma Y, Ota Y, Maruno T, Uza N, Uesugi M, Kageyama R, Chiba T, Seno H 2019 Hes1 plays an essential role in Kras-driven pancreatic tumorigenesis. *Oncogene* 38:4283-4296.
53. Liu A, Zhang D, Yang X, Song Y 2019 Estrogen receptor alpha activates MAPK signaling pathway to promote the development of endometrial cancer. *J Cell Biochem* 120:17593-17601.
54. Li TT, Liu MR, Pei DS 2019 Friend or foe, the role of EGR-1 in cancer. *Medical Oncology (Northwood, London, England)* 37:7.
55. Li L, Ameri AH, Wang S, Jansson KH, Casey OM, Yang Q, Beshiri ML, Fang L, Lake RG, Agarwal S, Alilin AN, Xu W, Yin JJ, Kelly K 2019 EGR1 regulates angiogenic and osteoclastogenic factors in prostate cancer and promotes metastasis. *Oncogene* 38:6241-6255.
56. Degl'Innocenti D, Romeo P, Tarantino E, Sensi M, Cassinelli G, Catalano V, Lanzi C, Perrone F, Pilotti S, Seregini E, Pierotti MA, Greco A, Borrello MG 2013 DUSP6/MKP3 is overexpressed in papillary and poorly differentiated thyroid carcinoma and contributes to neoplastic properties of thyroid cancer cells. *Endocr Relat Cancer* 20:23-37.
57. Ahmad MK, Abdollah NA, Shafie NH, Yusof NM, Razak SRA 2018 Dual-specificity phosphatase 6 (DUSP6): a review of its molecular characteristics and clinical relevance in cancer. *Cancer Biol Med* 15:14-28.
58. Longqiu Y, Pengcheng L, Xuejie F, Peng Z 2016 A miRNAs panel promotes the proliferation and invasion of colorectal cancer cells by targeting GABBR1. *Cancer Med* 5:2022-2031.
59. Lou I, Odorico S, Yu XM, Harrison A, Jaskula-Sztul R, Chen H 2018 Notch3 as a novel therapeutic target in metastatic medullary thyroid cancer. *Surgery* 163:104-111.

60. Huang Z, Cheng Y, Chiu PM, Cheung FMF, Nicholls JM, Kwong DL-W, Lee AWM, Zabarovsky ER, Stanbridge EJ, Lung HL, Lung ML 2012 Tumor suppressor Alpha B-crystallin (CRYAB) associates with the cadherin/catenin adherens junction and impairs NPC progression-associated properties. *Oncogene* 31:3709-3720.
61. Ruan H, Li Y, Wang X, Sun B, Fang W, Jiang S, Liang C 2020 CRYAB inhibits migration and invasion of bladder cancer cells through the PI3K/AKT and ERK pathways. *Jpn J Clin Oncol* 50:254-260.
62. Sun X, Zou T, Zuo C, Zhang M, Shi B, Jiang Z, Cui H, Liao X, Li X, Tang Y, Liu Y, Liu X 2018 IL-1 α inhibits proliferation and adipogenic differentiation of human adipose-derived mesenchymal stem cells through NF- κ B- and ERK1/2-mediated proinflammatory cytokines. *Cell Biol Int* 42:794-803.
63. Sigurdson AJ, Brenner AV, Roach JA, Goudeva L, Müller JA, Nerlich K, Reiners C, Schwab R, Pfeiffer L, Waldenberger M, Braganza M, Xu L, Sturgis EM, Yeager M, Chanock SJ, Pfeiffer RM, Abend M, Port M 2016 Selected single-nucleotide polymorphisms in FOXE1, SERPINA5, FTO, EVPL, TICAM1 and SCARB1 are associated with papillary and follicular thyroid cancer risk: replication study in a German population. *Carcinogenesis* 37:677–684.
64. Yin H, Meng T, Zhou L, Chen H, Song D 2017 SPC24 is critical for anaplastic thyroid cancer progression. *Oncotarget* 8:21884–21891.
65. Gao F, Huang W, Zhang Y, Tang S, Zheng L, Ma F, Wang Y, Tang H, Li X 2015 Hes1 promotes cell proliferation and migration by activating Bmi-1 and PTEN/Akt/GSK3 β pathway in human colon cancer. *Oncotarget* 6:38667-38680.
66. Li X, Cao Y, Li M, Jin F 2018 Upregulation of HES1 Promotes Cell Proliferation and Invasion in Breast Cancer as a Prognosis Marker and Therapy Target via the AKT Pathway and EMT Process. *J Cancer* 9:757-766.
67. Yamashita AS, Geraldo MV, Fuziwara CS, Kulcsar MA, Friguglietti CU, da Costa RB, Baia GS, Kimura ET 2013 Notch pathway is activated by MAPK signaling and influences papillary thyroid cancer proliferation. *Transl Oncol* 6: 197-205.
68. Lee J, Seol MY, Jeong S, Kwon HJ, Lee CR, Ku CR, Kang SW, Jeong JJ, Shin DY, Nam KH, Lee EJ, Chung WY, Jo YS 2015 KSR1 is coordinately regulated with Notch signaling and oxidative phosphorylation in thyroid cancer. *J Mol Endocrinol* 54:115-124.

69. Somnay YR, Yu XM, Lloyd RV, Levenson G, Aburjania Z, Jang S, Jaskula-Sztul R, Chen H 2017 Notch3 expression correlates with thyroid cancer differentiation, induces apoptosis, and predicts disease prognosis. *Cancer* 123:769-782.

Figure Legends

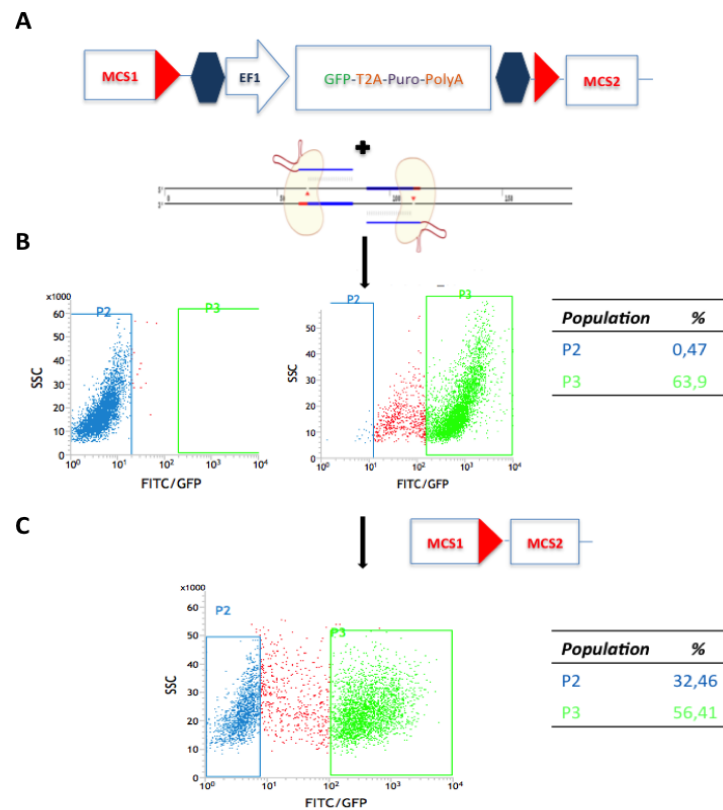


Figure 1.

Figure 1. Scheme of the vector employed for *LGALS3* gene editing, double nickase CRISPR/Cas9 vectors, and output of the FACS following the co-transfection with Lipofectamine 3000. After the co-transfection, cells integrating the portion of gene of interest and the marker cassette were sorted (P3=63.9%). P2 represents WT Nthy-Ori cells (P2=0.47%) after FACS. Edited cells were selected by sorting, Cre-loxed (for removing marker cassette) and sorted once again. In this last step, we collected only the edited cells depleted for the marker cassette (P2=32.46%).” (panel C).

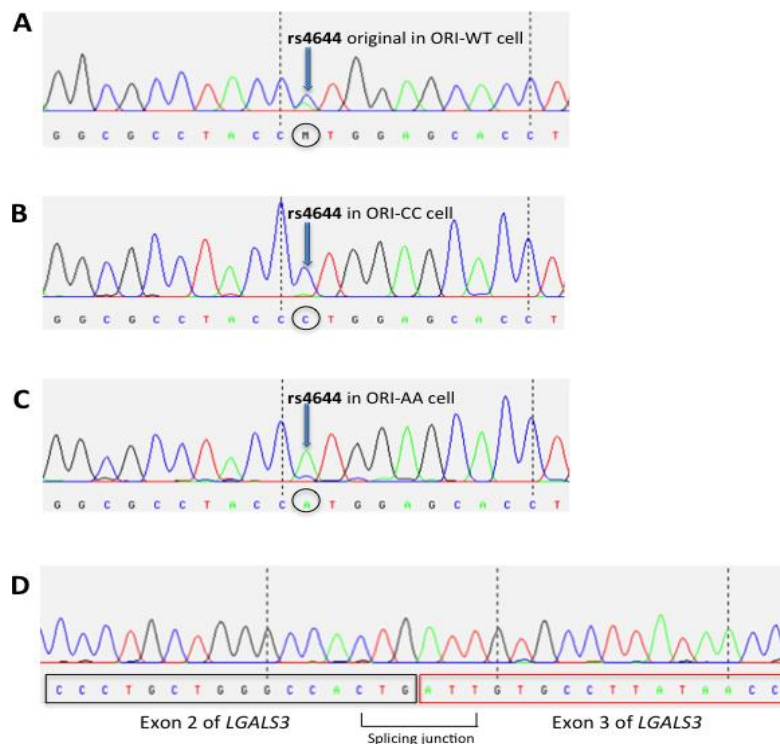


Figure 2.

Figure 2. Sanger sequencing electropherograms showing the gene editing (A, B and C) and splicing mechanism (D) in Nthy-Ori cell lines. The panel A shows the rs4644 in ORI-WT cell. The panel B and C show the results of the correct gene editing of rs4644 (ORI-CC and ORI-AA). The panel D shows the splicing junction between Exon 2 and Exon 3 that was not impaired by LoxP site residue.

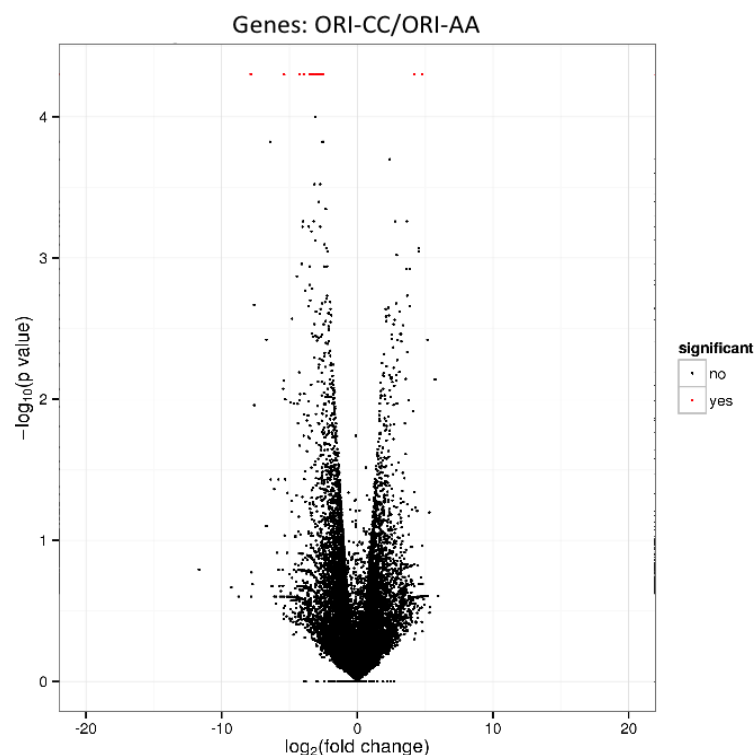


Figure 3

Figure 3. Volcano plot showing the relative expression (fold-change, Y-axis) of the genes measured in the ORI-AA and in ORI-CC cells and the statistical significance of the comparisons (X-axis). Genes showing a statistically significant different expression level between ORI-CC and ORI-AA cells are shown in red.

Thyroid

Pro64His (rs4644) polymorphism within galectin-3 is a risk factor of differentiated thyroid carcinoma and affects the transcriptome of thyrocytes engineered via CRISPR/Cas9 system. (DOI: 10.1089/thy.2020.0366)
This paper has been peer-reviewed and accepted for publication, but has yet to undergo copyediting and proof correction. The final published version may differ from this proof.

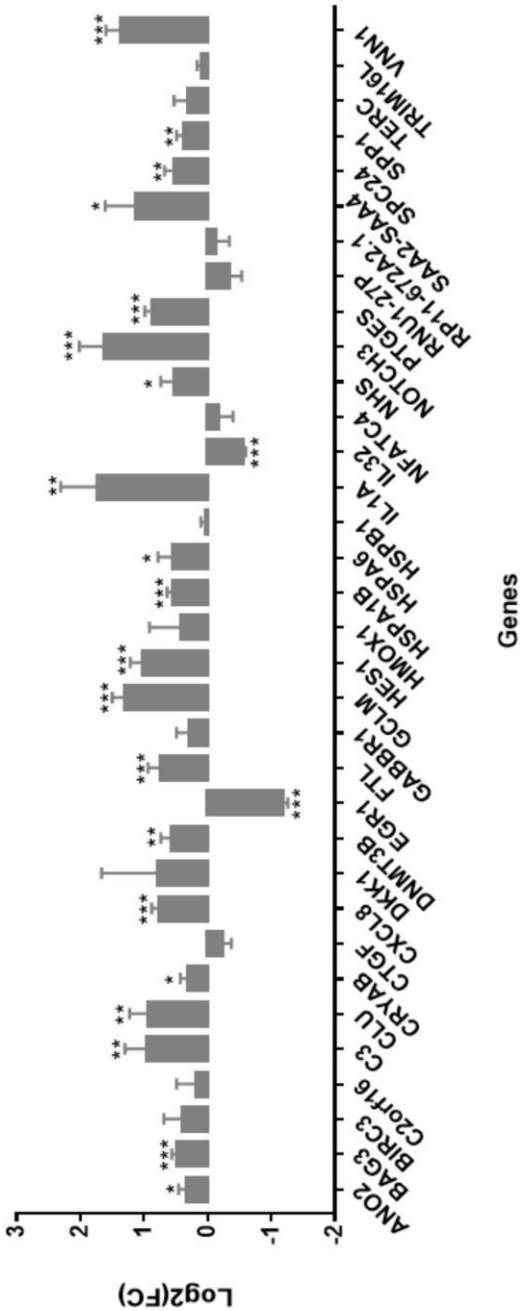


Figure 4

Figure 4. Genes differentially expressed between cells treated with siCtrl and siLGALS3 (* q-value<0.05; ** q-value<0.01; *** q-value<0.001).

Table 1. Main covariates of the population analysed in the case-control association study with their odd ratios (ORs) and confidence intervals (95% CI).

		OR (95% CI)	P _{ass}	Controls (1223)	Cases (1142)
Covariates					
<i>Age (years, average)</i>			<10 ⁻⁶	52.98	42.01
<i>BMI (average)</i>			0.20	25.86	26.80
<i>Sex</i>	Males	Reference		608 (49.7%)	310 (27.1%)
	Females vs Males	2.93 (2.53-3.79)	<10 ⁻⁶	615 (50.3%)	832 (72.9%)
<i>Smoking</i>	No	Reference		821 (67.2%)	690 (60.5%)
	Yes vs No	1.34 (1.13-1.59)	8.00x10 ⁻⁴	402 (32.8%)	452 (39.5%)
<i>Histotype</i>	PTC				1056 (92.5%)
	FTC				86 (7.5%)
Genotype				DTC (1142)	
<i>rs4644</i>	C/C	Reference		577 (47.2%)	595 (52.1%)
	C/A vs C/C	0.89 (0.74-1.08)	0.23	536 (43.8%)	473 (41.4%)
	A/A vs C/C	0.66 (0.46-	0.02	110	74

	0.93)		(8.99%)	(6.48%)
Allele A vs C	0.83 (0.74- 0.95)	4.9x10 ⁻³	756 (30.9%)	621 (27.3%)

Trend-test for co-dominance: $\chi^2=8.189$; $P_{\text{trend}}=4.21 \times 10^{-3}$

				PTC (1056)
C/C	Reference		577 (47.2%)	555 (52.6%)
C/A vs C/C	0.88 (0.73- 1.06)	0.18	536 (43.8%)	431 (40.8%)
A/A vs C/C	0.67 (0.47- 0.96)	0.03	110 (8.99%)	70 (6.63%)
Allele A vs C	0.82 (0.73- 0.94)	4.1x10 ⁻³	756 (30.9%)	571 (27%)

Trend-test for co-dominance: $\chi^2=21.2$; $P_{\text{trend}}=4.11 \times 10^{-6}$

				FTC (86)
C/C	Reference		577 (47.2%)	40 (46.5%)
C/A vs C/C	1.17 (0.73- 1.88)	0.52	536 (43.8%)	42 (48.8%)
A/A vs C/C	0.49 (0.17- 1.43)	0.19	110 (8.99%)	4 (4.68%)
Allele A vs C	0.92 (0.65- 1.29)	0.61	756 (30.9%)	50 (29%)

Trend-test for co-dominance: $\chi^2=0.26$; $P_{\text{trend}}=0.61$

BMI: Body mass index; DTC: Differentiated Thyroid Carcinoma; PTC: Papillary Thyroid Carcinoma; FTC: Follicular Thyroid Carcinoma.

According to the co-dominant model, the table reports the calculated ORs and 95% CI of the *LGALS3*-rs4644 genotypes C/A and A/A versus the reference (the common homozygotes C/C) adjusted for the covariates and the results of the MAX trend tests. Association analyses were provided for the total DTC samples and for the sub-sets of PTC and FTC histotypes.

Table 2. List of 39 differentially expressed genes in ORI-AA and ORI-CC cells selected for further validation and experimentation according to the criteria specified in the text. Group A and Group B included genes overexpressed in ORI-AA or ORI-CC. Genes in Group C are involved in thyroid carcinogenesis, in group D are listed genes with the highest differential expression. For each sample, the genes are listed with the expression values in fragment per kilobase per million mapped reads (FPKM).

<i>Gene</i>	<i>FPKM_ORI_A</i>	<i>FPKM_ORI_C</i>	<i>log2(Fold- Change)(FC)</i>	<i>p-value</i>	<i>q- value</i>
<i>A</i>	<i>C</i>				
(Group A)					
BAG3	205.15	32.90	-2.64	5.00x10 ⁻⁵	0.0446
BIRC3	7.87	0.51	-3.95	5.00x10 ⁻⁵	0.0446
C3	325.85	39.71	-3.04	5.00x10 ⁻⁵	0.0446
CLU	276.01	38.58	-2.84	5.00x10 ⁻⁵	0.0446
CXCL8	178.14	15.50	-3.52	5.00x10 ⁻⁵	0.0446
FTL	3786.91	489.43	-2.95	5.00x10 ⁻⁵	0.0446
GABBR1	9.69	* 10 ⁻⁶	<-20	5.00x10 ⁻⁵	0.0446
GCLM	57.39	8.84	-2.70	5.00x10 ⁻⁵	0.0446
HMOX1	2336.87	10.15	-7.85	5.00x10 ⁻⁵	0.0446
HSPA1B	5.16	* 10 ⁻⁶	<-20	5.00x10 ⁻⁵	0.0446
HSPB1	978.75	101.71	-3.27	5.00x10 ⁻⁵	0.0446

Thyroid

					29
				⁵	
HSPB8	1.62	$\ast 10^{-6}$		5.00x10 ⁻	0.0446
			<-20	⁵	
IL32	105.90	2.52		5.00x10 ⁻	0.0446
			-5.39	⁵	
NFATC4	5.59	0.29		5.00x10 ⁻	0.0446
			-4.27	⁵	
PTGES	170.24	20.18		5.00x10 ⁻	0.0446
			-3.08	⁵	
RNU1-27P	5.41	$\ast 10^{-6}$		5.00x10 ⁻	0.0446
			<-20	⁵	
RP11-672A2.1	5.97	$\ast 10^{-6}$		5.00x10 ⁻	0.0446
			<-20	⁵	
SAA2-SAA4	3.06	$\ast 10^{-6}$		5.00x10 ⁻	0.0446
			<-20	⁵	
SPP1	1.66	$\ast 10^{-6}$		5.00x10 ⁻	0.0446
			<-20	⁵	
TRIM16L	82.86	5.34		5.00x10 ⁻	0.0446
			-3.96	⁵	
VNN1	2.14	$\ast 10^{-6}$		5.00x10 ⁻	0.0446
			<-20	⁵	
<hr/>					
(Group B)					
ANO2	$\ast 10^{-6}$	3.57		5.00x10 ⁻	0.0446
			>20	⁵	
EGR1	12.17	331.21		5.00x10 ⁻	0.0446
			4.77	⁵	
HES1	7.52	137.83		5.00x10 ⁻	0.0446
			4.20	⁵	
<hr/>					

30

(Group C)

NOTCH3	15.15	1.78		1.00x10 ⁻⁴	0.0841
			-3.09		
DNMT3B	73.12	12.22		1.50x10 ⁻⁴	0.1052
			-2.58		
CTGF	79.05	410.70		2.00x10 ⁻⁴	0.1155
			2.38		
CRYAB	141.78	15.21		5.50x10 ⁻⁴	0.1785
			-3.22		
IL1A	1.77	* 10 ⁻⁶		5.50x10 ⁻⁴	0.1785
			<-20		
TERC	1.40	* 10 ⁻⁶		6.00x10 ⁻⁴	0.1785
			<-20		
TNFAIP6	2.41	* 10 ⁻⁶		8.00x10 ⁻⁴	0.1963
			<-20		
DKK1	45.89	9.44		8.50x10 ⁻⁴	0.2052
			-2.28		

(Group D)

C2orf16	0.09	0.96	3.42	0.2179	0.9850
CTB-32H22.1	5.20	0.37	-3.81	0.2687	0.9850
DUSP6	0.32	4.01	3.65	0.4308	0.9850
HSPA6	94.86	0.03	-11.63	0.1617	0.9850
NHS	2.27	0.19	-3.58	0.2765	0.9850
SPC24	18.56	0.75	-4.63	0.2517	0.9850
SPATA5	0.28	2.56	3.19	0.3012	0.9850

- * These genes showed an almost negligible expression not allowing to perform any calculation.

The values have been replaced with a minimal number (10^{-6}) to allow a rough estimate (denoted with the signs "<" or ">") of the fold-change.

Table 3. List of 34 genes analysed by real-time qPCR. The statistically significance is referred to the linear regression model using the allele dosage of rs4644 as independent variable being ORI-AA = 0, ORI-WT=1, and ORI-CC=2 variant alleles. The model is reported as intercept, slope and standard error (se) of the slope.

<i>Gene</i>	Intercept	Slope (\pm se)	p-value
<i>ANO2</i>	2.23	-0.11 \pm 0.31	0.743
<i>BAG3</i>	-0.88	0.39 \pm 0.01	<10 ⁻⁶
<i>BIRC3</i>	-2.27	0.37 \pm 0.09	0.009
<i>C3</i>	-0.79	0.44 \pm 0.03	<10 ⁻⁶
<i>CLU</i>	-1.01	0.48 \pm 0.06	<10 ⁻⁶
<i>CXCL8</i>	-1.35	0.41 \pm 0.01	<10 ⁻⁶
<i>EGR1</i>	2.54	-0.21 \pm 0.05	6.00x10 ⁻⁴
<i>FTL</i>	0.68	0.40 \pm 0.03	<10 ⁻⁶
<i>GABBR1</i>	-0.96	0.19 \pm 0.21	0.379
<i>GCLM</i>	-1.70	0.47 \pm 0.06	<10 ⁻⁶
<i>HES1</i>	6.41	-0.63 \pm 0.08	<10 ⁻⁶
<i>HMOX1</i>	0.17	0.15 \pm 0.03	<10 ⁻⁶
<i>HSPA1B</i>	-0.51	0.36 \pm 0.02	<10 ⁻⁶
<i>HSPB1</i>	0.04	0.33 \pm 0.04	<10 ⁻⁶
<i>IL32</i>	-4.38	0.56 \pm 0.14	5.00x10 ⁻⁴
<i>NFATC4</i>	-5.62	0.53 \pm 0.14	0.001
<i>PTGES</i>	-2.43	0.51 \pm 0.04	<10 ⁻⁶
<i>RNU1-27P</i>	-0.66	0.90 \pm 0.19	2.00x10 ⁻⁴
<i>RP11-672A2.1</i>	-1.96	0.28 \pm 0.21	0.189
<i>SAA2-SAA4</i>	-0.69	0.20 \pm 0.02	<10 ⁻⁶
<i>SPP1</i>	-10.33	0.71 \pm 0.27	0.014
<i>TRIM16L</i>	-4.86	0.80 \pm 0.08	<10 ⁻⁶
<i>VNN1</i>	-5.76	0.53 \pm 0.07	<10 ⁻⁶
<i>NOTCH3</i>	-2.95	0.36 \pm 0.04	<10 ⁻⁶
<i>DNMT3B</i>	-2.29	0.38 \pm 0.03	<10 ⁻⁶

			33
CTGF	3.52	-0.31±0.14	0.036
CRYAB	-2.41	0.35±0.07	<10 ⁻⁶
IL1A	-0.54	0.19±0.03	<10 ⁻⁶
TERC	-3.93	0.77±0.14	<10 ⁻⁶
DKK1	-2.60	0.30±0.09	0.005
C2orf16	1.48	-0.05±0.13	0.712
HSPA6	-0.48	0.18±0.04	<10 ⁻⁶
NHS	0.05	0.08±0.13	0.515
SPC24	-2.47	0.38±0.12	0.003

34

HSPA1B	5.16	1.79	*1.00x	<-	5.00x	1.4	0.127	<-20	5.00x
			10⁻⁶	20	10⁻⁵	6			10⁻⁵
HSPB1	978.	441.18	101.7	-	5.00x	1.0	0.059	-2.18	0.001
	75		1	3.27	10 ⁻⁵	9			
HSPB8	1.62	0.42	*1.00x	<-	5.00x	1.8	0.137	<-15	0.004
			10 ⁻⁶	20	10 ⁻⁵	8			
IL32	105.	13.39	2.52	-	5.00x	2.9	1.00x	-2.47	0.009
	90			5.39	10 ⁻⁵	2	10 ⁻⁴		
NFATC4	5.59	4.36	0.29	-	5.00x	0.3	0.625	-3.94	4.50x
				4.27	10 ⁻⁵	0			10 ⁻⁴
PTGES	170.	53.36	20.18	-	5.00x	1.6	0.002	-1.46	0.020
	24			3.08	10 ⁻⁵	1			
RNU1-	5.41	0.15	*1.00x	<-	5.00x	5.1	0.242	<-15	1.000
27P			10 ⁻⁶	20	10 ⁻⁵	1			
RP11-	5.97	0.34	*1.00x	<-	5.00x	4.0	0.015	<-15	0.004
672A2.1			10 ⁻⁶	20	10 ⁻⁵	7			
SAA2-	3.06	0.54	*1.00x	<-	5.00x	2.4	0.030	<-15	4.50x
SAA4			10 ⁻⁶	20	10 ⁻⁵	4			10 ⁻⁴
SPP1	1.66	0.03	*1.00x	<-	5.00x	5.7	0.215	<-15	1.000
			10 ⁻⁶	20	10 ⁻⁵	3			
TRIM16L	82.8	26.56	5.34	-	5.00x	1.5	0.003	-2.38	0.003
	6			3.96	10 ⁻⁵	8			
VNN1	2.14	*1.00x	*1.00x	<-	5.00x	>2	1.00x	Undeter	1.000
		10 ⁻⁶	10 ⁻⁶	20	10 ⁻⁵	0	10 ⁻⁴	mined	
NOTCH3	15.1	17.57	1.78	-	1.00x	-	0.566	-3.37	5.00x
	5			3.09	10 ⁻⁴	0.2			10 ⁻⁵
						8			
DNMT3B	73.1	20.82	12.22	-	1.50x	1.7	0.001	-0.83	0.191
	2			2.58	10 ⁻⁴	5			
CTGF	79.0	77.22	410.7	2.38	2.00x	-	0.954	2.35	8.50x

	5	0	10 ⁻⁴	0.0	10 ⁻⁴	35
				3		
CRYAB	141.	54.22	15.21	-	5.50x	1.3 0.017 -1.90 0.013
	78		3.22	10 ⁻⁴	2	
IL1A	1.77	*1.00x	*1.00x	<-	5.50x	>2 7.00x Undeter 1.000
		10 ⁻⁶	10 ⁻⁶	20	10 ⁻⁴	0 10 ⁻⁴ mined
TERC	1.40	0.23	*1.00x	<-	6.00x	2.5 0.169 <-15 1.000
			10 ⁻⁶	20	10 ⁻⁴	4
TNFAIP6	2.41	0.12	*1.00x	<-	8.00x	4.2 0.246 <-15 1.000
			10 ⁻⁶	20	10 ⁻⁴	7
DKK1	45.8	16.11	9.44	-	8.50x	1.4 0.005 -0.83 0.179
	9		2.28	10 ⁻⁴	5	
C2orf16	0.09	0.13	0.96	3.42	0.218	- 1.000 2.85 0.181
					0.5	
					3	
CTB-	5.20	1.84	0.37	-	0.269	1.4 0.386 -2.38 0.382
32H22.1				3.81		4
DUSP6	0.32	*1.00x	4.01	3.65	0.431	>1 1.000 >20 0.212
		10 ⁻⁶				5
HSPA6	94.8	6.45	0.03	-	0.162	3.8 1.00x -7.78 0.149
	6		11.6			2 10 ⁻⁴
			3			
NHS	2.27	*1.00x	0.19	-	0.277	>2 0.004 >15 1.000
		10 ⁻⁶	3.58			0
SPC24	18.5	2.97	0.75	-	0.252	2.5 0.164 -2.05 0.427
	6		4.63			8
SPATA5	0.28	*1.00x	2.56	3.19	0.301	>1 0.134 >20 0.210
		10 ⁻⁶				5

* These genes showed an almost negligible expression not allowing to perform any calculation.

The values have been replaced with a minimal number (10^{-6}) to allow a rough estimate (denoted with the signs “<” or “>”) of the fold-change.